The Local Web Buckling Strength of Coped Steel I-Beam

Michael C. H. Yam[1] Member, ASCE
Angus C. C. Lam[2] Associate Member, ASCE,
V. P. IU[2] and J. J. R. Cheng[3] Members, ASCE

ABSTRACT : When a beam flange is coped to allow clearance at the connection, the strength of the coped region will be reduced. Local web buckling at the coped region may occur when the cope length is long and/or the compression flange is braced. Experimental and analytical investigation of the strength of coped steel I-beams were conducted by a number of researchers and design formula were also proposed. However, the proposed formula underestimate the local web buckling capacity of coped I-beam especially when the cope depth to beam depth ratio is small. To improve this discrepancy, full-scale tests of the web buckling strength of coped steel I-beams and a series of analytical studies were carried out. A modified plate buckling formulae, which considers the shear buckling phenomenon at the coped region, is proposed. The modified formulae gives better prediction of the local web buckling strength of coped I-beam. The test-to-predicted ratios varies from 0.92 to 1.06.

---

[1] Dept. of Building & Real Estate, The Hong Kong Polytechnic University, Hung Hum, Kowloon, Hong Kong
(Tel: (852) 2766 4380 Fax: (852) 2764 5131 Email: bsmyam@polyu.edu.hk)
[2] Faculty of Science & Technology, University of Macau, P.O. Box 3001, Macau
[3] Dept. of Civil and Environmental Engineering, University of Alberta, Edmonton, Alberta, Canada

INTRODUCTION

In steel construction, when beams have to be connected at the same elevation, beam flanges must often be coped to provide enough clearance for the supports. The cope can be at the top (as shown in Fig. 1), the bottom or both flanges in combination. When the beam flanges are coped, the lateral-torsional buckling capacity and the local web buckling capacity of the beam may be reduced. Investigation on the connection behavior at copes of stocky web beams was studied by Birkemoe and Gilmor (1978), and Ricles and Yura (1980). The block shear failure mode was identified by the studies. For thin webs, failure could occur by local web buckling at the coped region. Theoretically, the buckling load could be much lower than the yield stress. Cheng et al. (1984) carried out the investigation of coped steel I-beams extensively by both experimental and analytical studies. The effects of cope length, cope depth, cross-sectional geometry, and span length on the local web buckling as well as lateral torsional buckling capacities were investigated. Design formula were proposed and presented by Cheng et al. (1984). Further studies of the design and behavior of coped I-beams were also conducted by Cheng and his co-researchers (Cheng and Yura 1986, Cheng and Yura 1988, Yam and Cheng 1990, Cheng and Snell 1991, Cheng 1993, Lam et al. 2000, Yam et al. 2000). In this paper, experimental studies of the effect of coped depth (d_c) to beam depth (D) ratio on the local web buckling strength of coped steel I-beam are presented. Four full-scale coped steel I-beams with d_c/D varying from 0.05 to 0.3 were tested. Finite

element analysis of all the test specimens is also included in this paper. The local web buckling loads of the test specimens were compared with the predictions by both the finite element analysis and Cheng's equation (1984).

TEST PROGRAM

A total of four tests were conducted to study the local web buckling (LWB) behavior of top flange coped I-beams. Welded beam sections equivalent to UB406 x 140 x 39 and UB457 x 152 x 52 (BS5950, 1990) were used as the test specimens. These two sections are equivalent to the U.S. sections W16 x 26 and W18 x 35, respectively. The measured beam depth and the coped dimensions of the specimens are shown in Table 1. The ratio of cope depth to beam depth (d_c/D) varies from 0.05 to 0.3. These ratios are also indicated in the specimen designation, i.e. 406d01 represents UB406 x 140 x 39 section with d_c/D equal to 0.1. A single end plate was welded perpendicular to the beam web to be connected to the reaction wall. The size of the end plates were designed to provide enough shear strength and at the same time minimized the plates' in-plane rotational stiffness in order to simulate a simply supported boundary condition for the coped beam end. Typical cope details and the dimensions of the end plate for 406d005 are shown in Fig. 2. With this design boundary condition and cope length, elastic local web buckling of the test specimens was expected. Tension coupons were prepared from the test beam webs in the longitudinal direction and tested according to ASTM A370 standard (1997). The

average tensile yield strength of the web was 343 MPa and the average elastic modulus of the web was 216,600 MPa.

The test setup is shown schematically in Fig. 3, along with a sketch of test specimens. The specimens were tested up side down with the load applied to the specimen vertically upward. The load position was chosen not only to produce failure in the coped region but also to minimize the effect of the load itself on the stress distribution in the coped region. The distance from the load position to the end plate was 995 mm (2.5D) for specimens 406d005, 406d01 and 406d03 and 1125 mm (2.5D) for 457d02, as shown in Fig. 3. Lateral bracings were provided close to the load and reaction, and at the compression flange close to the end of the cope in order to prevent lateral movement, as shown in Fig. 3. Since the local web buckling is a local behavior, the other end of each specimen was used as another test once the end that was connected to the strong wall failed.

Load was applied quasi-statically and was controlled by an electro-hydraulic servo controller. Load cells were used to record the load and reaction applied to the specimens. For measuring the in-plane deflections, dial gauges were set up at the load position and at the end of the cope. Another set of dial gauges was set up on the web to measure the lateral deflection. In addition, longitudinal

strain gauges were mounted on the web at the cope to measure the strains of the web at cope and to detect buckling of the web.

The test procedure was generally the same for all the tests. The loading procedure was divided into two stages. In the first stage, load was applied by controlling the magnitude of the loading (i.e. load control). After the applied load reached approximately 50% of the expected maximum load, load was then applied by controlling the magnitude of the vertical deflection at the load point (i.e. stroke control). Load was applied until the post-buckling curve was obtained.

EXPERIMENTAL RESULTS

The general failure mode of the specimens was local web buckling at the cope region. The ultimate loads, P_{Test}, of all the specimens are shown in Table 2. The test results show that when d_c/D increases, the ultimate load of the specimens decreases. The load versus in-plane vertical deflection curves (Fig. 4) show that a linear load-deflection behavior exists before local web buckling occurs. This indicates that these four specimens did not experience significant yielding prior to instability failure.

Strain readings at the junction of I-section and T-section (cope region) of specimens 406d005 and 406d03 are shown in Figs. 5a and 5b, respectively, with

three different load levels (about 40%, 80%, and 96% of ultimate load). The centroidal axes of the I-section and the T-section are also included in the figures. It can be seen that the longitudinal strain across the depth of the section varies non-linearly at this junction. Strain readings at the cope corner are much higher than the calculated values using the T-section cross-sectional properties. This is mainly caused by the stress concentration at the cope corner. The neutral axis at this section is closer to the centroidal axis of I-section for specimen 406d005; however, the location of the neutral axis is closer to the centroidal axis of T-section for specimen 406d03. The bending stresses acting at the coped region, therefore, are higher for the specimen with small cope depth (406d005) and smaller for the specimen with large cope depth (406d03), as shown in Fig. 5. In other words, the stress concentration is not as significant for the specimen with large cope depth but is significant for the specimen with small cope depth.

A typical out-of-plane deflection plot of the web at the cope corner versus the applied load of specimen 406d03 is shown in Fig. 6. It can be seen that insignificant out-of-plane web deflection at the cope corner was observed when the applied load was lower than 50% of the ultimate load. When the ultimate load was reached significant lateral deflection was observed.

FINITE ELEMENT ANALYSIS OF TEST SPECIMENS

The test specimens were analyzed by the finite element method using the finite element program, ABAQUS (1997). Shell elements with six degrees of freedom at each node were used to model the test beams. Typical model of the test beam is shown in Fig. 7. To simplify the finite element model, roller support was placed at the neutral axis of the I-section. A point load was used to model the applied load since the contact area between the hydraulic ram and the specimen was relatively small. In the finite element model, the overhang part of the beam was not included in the model since it had no influence to the coped region. Tri-linear material stress-strain curve according to the tensile coupon test results was used in the material modeling. The load-deflection analysis included both the material and geometric nonlinearities. To consider the geometric non-linear effect, initial imperfection, which was based on the first mode of the local web buckling at the cope, was used in the non-linear analysis. Since the out-of-plane imperfection was not measured during the test, suitable values of imperfection were assigned in the finite element analysis in order to capture the load-deflection behavior of the specimens. The maximum initial imperfection e, as shown in Fig. 4, used in this analysis was 1 mm. The initial imperfection values used in the different specimens (e = 0.2 mm to 1.0 mm as indicated in Fig. 4) have little effect on the final load-deflection behavior of the specimens. This initial imperfection was less than the limit of the maximum tolerance on web plate that was specified in BS5950 (Part 2, Section 7, 1990).

COMPARISON OF FINITE ELEMENT RESULTS AND TEST RESULTS

The comparison of the buckling loads obtained by the finite element analyses and the test results are shown in Table 2. The test to predicted ratio (P_{FEM}/P_{Test}) varies from 0.95 to 1.01 with a mean value of 0.99. The load versus in-plane deflection curves of the specimens from the finite element analysis were compared with the test results as shown in Fig. 4. For specimens 406d005 and 406d01, the post buckling behavior of the analytical results were more stable than that of the test results. However, for the other specimens, the analytical load (loading and unloading) versus deflection curves compared well with the test results. Typical buckled shapes at cope line of specimen 406d01 and 406d005 of the test and the analytical results are shown in Figs. 8 and 9. Figure 8 shows the bottom view of the coped section. Both the test and analytical results showed that maximum lateral deflection occurred at the cope line.

COMPARISON OF TEST RESULTS WITH PRESENT DESIGN METHODS

According to British Constructional Steelwork Association limited (BCSA, 1993), it is stated that no stability check of coped end is needed when the cope length (c) is less than $110000D / (D/t_w)^3$, where D is the beam depth and t_w is the web thickness for $D/t_w > 48$ (Grade 50 steel, $\sigma_y \geq 325$ MPa). Otherwise,

stability of web should be checked according to the equations proposed by Cheng et al. (1984). Since the cope length of all the specimens were larger than $110000D / (D/t_w)^3$ in this study, the corresponding local web buckling capacity of the coped end were calculated according to the following equations proposed by Cheng et al. (1984).

$$\sigma_{cr} = f \frac{k\pi^2 E}{12(1-\nu^2)} \left(\frac{t_w}{h_o} \right)^2 \tag{1}$$

where E = modulus of elasticity, f = adjustment factor, k = plate buckling coefficient, h_o = height of web of T-section, t_w = web thickness, σ_{cr} = plate critical stress, and ν = Poisson's ratio.

The plate buckling coefficient (k) and the adjustment factor (f) are defined as follows:

$$\begin{aligned} k &= 2.2 \left(\frac{h_o}{c} \right)^{1.65} && \text{for} \quad \frac{c}{h_o} \le 1.0 \\ k &= 2.2 \left(\frac{h_o}{c} \right) && \text{for} \quad \frac{c}{h_o} > 1.0 \end{aligned} \tag{2}$$

and

$$\begin{aligned} f &= \frac{2c}{D} && \text{for} \quad \frac{c}{D} \le 1.0 \\ f &= 1 + \frac{c}{D} && \text{for} \quad \frac{c}{D} > 1.0 \end{aligned} \tag{3}$$

It should be noted that the critical stress, σ_{cr}, should not be greater than the static yield stress, σ_y, of the material. The end plate reaction (R_{Cheng}) corresponding to

the critical local web buckling stress, σ_{cr}, were calculated and compared with the test results (R_{Test}). Consequently, the reaction corresponding to the shear yield capacity ($R_{vy} = 0.6\sigma_y \times 0.9h_o t_w$) and flexural yield capacity ($R_y = \sigma_y S_{Tee}/c$) were calculated according to BS5950 (1990) with the actual material strength and the results are summarized in Table 2. It can be seen from the table that when d_c/D is small (<0.2), Cheng's equation (R_{Cheng}) gives conservative prediction. The test-to-predicted ratios for specimens 406d005 and 406d01 are 1.23 and 1.27, respectively. Hence, further study on Cheng's equation for the prediction of the local web buckling capacity of coped beam was carried out to reduce the conservatism for small d_c/D values.

Cheng et al. (1984) suggested that the buckling line in the web should be oriented at about 45 degree angle from a vertical line if shear stresses dominated the buckling behavior. The test and analytical results from this study also showed that the buckling line inclined at an angle when the cope length was short (Fig. 9). Therefore, it was believed that shear stresses dominated the buckling behavior when the ratio of cope length to the reduced beam depth was small ($c/h_o < 1.5$). In Cheng's equation (Eq. 1), the influence of shear stress, cope depth, and moment variation from the beam end to the end of the cope was considered by a single adjustment factor, f. The use of this factor, f, might be conservative since only three variables were used in the derivation of the equation for the adjustment factor f.

STUDY OF SHEAR STRESSES AT THE COPE

Typical finite element results of the shear stress distribution at the flange/web junction are shown in Fig. 10. Theoretical values of the shear stress based on the conventional mechanics of materials at the coped (or T-) section and the uncoped (or I-) section are also shown in the same figure for comparison. As expected, when an I-beam is coped, the shear stress of the coped section at the junction of the web to the flange will become larger than that of the I-section due to the shape change at the cope. On the other hand, in order to maintain equilibrium of horizontal forces, shear stress at the compression top flange/web junction of I-section will become larger than the theoretical value. The ratio of the shear stress at the cope (τ_T) and I-section (τ_I) at the bottom flange/web junction is approximately equal to

$$m = \frac{I_I}{I_T}\left(\frac{2\bar{y}}{D}\right) \tag{4}$$

where

$m = \tau_T/\tau_I$ at the bottom flange/web junction

I_I = moment of inertia of the I-section

I_T = moment of inertia of the T-section

$\bar{y}$ = centroidalal axis of the T-section measured from the extreme fiber of the flange

D = beam depth

It is obvious that the factor m is related to the dimension of the I-beam and the cope depth. Hence, a whole range of beams was studied in order to obtain a range of m values with d_c/D varied from 0.05 to 0.5. It can be seen in Fig. 11 that the variation of m is small (about 6%) for different beam sections when d_c/D is constant. On the other hand, the factor m increases as d_c/D increases.

PROPOSED MODIFIED PLATE EQUATION

Based on the above study, a modified plate model with boundary conditions and stresses shown in Fig. 12 is proposed to predict the LWB strength of coped I-beams. The average m values, which are obtained from Fig. 11, are related to d_c/D as follows

$$m = 6.6\left(\frac{d_c}{D}\right)^2 + 0.4\left(\frac{d_c}{D}\right) + 1.4 \qquad (5)$$

where $0.05 \le d_c / D \le 0.5$

It should be noted that the bending stress at the uncoped section was not included in the model. As it was discussed before, when the cope length to the reduced beam depth ratio was small, shear stress would dominate the buckling behavior of coped section. Therefore, the influence of bending stress at the uncoped section to the local web buckling strength at cope section was believed to be small. To verify this assumption, finite element studies of the plate model with bending and shear stresses as the boundary stresses were also conducted

and it was found that the results of the plate model with bending and shear stresses were only 4% larger than the results of the plate model with shear stress only. Hence, it was decided to use the modified plate model with shear stress only since it gave conservative prediction and the model would be simpler.

Studies of the modified plate model (Fig. 12) were carried out with main parameters including cope length, cope depth and thickness of the plate. The depth of the plate (D) was assigned to be 400 mm. The ratio of cope length to the plate depth (c/D) was varied from 0.1 to 1.5 and cope depth to plate depth ratio (d_c/D) was varied from 0.05 to 0.5. It should be noted that, in order to minimize the boundary effect, the length of the plate was changed from 2c to D when c/D was less than 0.5. The critical reactions obtained from the finite element analysis of the modified plate model with plate thickness equal to 6 mm are shown in Fig. 13. Five curves with different d_c/D values are shown in the figure. It can be seen that for a constant value of d_c/D, the critical reaction decreases as c/D increases. On the other hand, the figure shows that the critical reaction decreases as d_c/D increases. It is obvious that increasing both cope length and cope depth would cause the buckling strength of the plate to decrease.

Based on the parametric study, it is proposed to develop a relatively simple design procedure to design the local web buckling strength of coped beams. As

it was also stated in previous section, Cheng et al. (1984) proposed a plate buckling equation to predict the critical bending stress at cope corner for predicting the LWB strength of coped I-beam. Two factors, k and f, which were related to the cope length to reduced beam depth ratio (c/h_o) and cope length to beam depth ratio (c/D), were introduced in the plate buckling equation. For a plate subjected to shear stress as the boundary stress, the following equation could be used to obtain the critical shear stress.

$$\tau_{cr} = k_s \frac{\pi^2 E}{12(1-\nu^2)}\left(\frac{t}{a_T}\right)^2 \tag{6}$$

where k_s = shear buckling coefficient

E = elastic modulus

ν = Poisson's ratio

t = thickness of plate

a_T = transverse length of plate

The aspect ratio of the cope region (c/h_o) was selected as the primary variable for obtaining the shear buckling coefficient, k_s, for a given d_c/D value. It is known that the shear buckling coefficient, k_s, is not only related to the aspect ratio but also related to the boundary conditions and applied stresses. Therefore, studies of the shear buckling coefficient, k_s, for a constant value of d_c/D were carried out. For a given d_c/D value, Eq. 6 was rewritten in the following form

$$\tau_{cr} = k_s \frac{\pi^2 E}{12(1-\nu^2)}\left(\frac{t_w}{h_o}\right)^2 \tag{7}$$

where k_s = shear buckling coefficient

E = elastic modulus

ν = Poisson's ratio

t_w = thickness of web

h_o = height of web of T-section

The above equation (Eq. 7) was rearranged in the following form to obtain the shear buckling coefficient

$$k_s = \tau_{cr} \frac{12(1-\nu^2)}{\pi^2 E}\left(\frac{h_0}{t_w}\right)^2 \quad (8)$$

The critical shear stresses (τ_{cr}) which were obtained from the finite element analysis of the modified plate model (Fig. 12) were then used to evaluate the shear buckling coefficients, k_s of Eq. 8.

The plot of the shear buckling coefficients, k_s, versus c/h_o for five different values of d_c/D are shown in Fig. 14 (a to e). As expected, the shear buckling coefficient, k_s, decreases as c/h_o increases. On the other hand, the shear buckling coefficient, k_s, decreases as d_c/D increases for a constant value of c/h_o. It should be noted that the evaluation of the above shear buckling coefficient, k_s, was based on the plate with web thickness of 6 mm. Therefore, the depth to thickness ratio (D/t_w) equals to 66.7. It is obvious that the thickness of the plate will affect the boundary condition, such as the lateral stiffness and rotational stiffness at the junction of T-section and I-section. The change in boundary

condition may have influence on evaluating the shear buckling coefficient, k_s. Therefore, a finite element analysis of the modified plate model with different D/t_w value was investigated in order to obtain the influence of the plate thickness to the shear buckling coefficient, k_s. The ratio of D/t_w was varied from 66.7 to 25 with different combinations of d_c/D (0.1, 0.3 and 0.5) and c/D (0.5, 1 and 1.5). The finite element results showed that similar results were obtained for different d_c/D ratios even D/t_w values were different. It was found that the shear buckling coefficient, k_s, with D/t_w equal to 66.7 (t_w = 6 mm) was about 2% less than the shear buckling coefficient, k_s, with D/t_w equal to 25 (t_w = 16 mm). Since the difference of the shear buckling coefficient with respect to different values of D/t_w was small, the minimum values of k_s (corresponding to D/t_w = 66.7) were used in the following section.

Based on the above results, it was proposed to obtain a set of simple equations to express the relationship between the aspect ratio of the cope region (c/h_o) and the shear buckling coefficient, k_s. Therefore, the following equations with power order form were used to express the relation between the shear buckling coefficients, k_s, and (c/h_o) for a fixed value of d_c/D.

$$k_s = 1.31\left(\frac{h_o}{c}\right)^{1.38} \qquad \text{for } d_c/D = 0.05 \qquad (9a)$$

$$k_s = 1.21\left(\frac{h_o}{c}\right)^{1.29} \qquad \text{for } d_c/D = 0.1 \qquad (9b)$$

$$k_s = 1.0\left(\frac{h_o}{c}\right)^{0.98} \qquad \text{for } d_c/D = 0.2 \qquad (9c)$$

$$k_s = 0.8\left(\frac{h_o}{c}\right)^{0.9} \qquad \text{for } d_c/D = 0.3 \qquad (9d)$$

$$k_s = 0.51\left(\frac{h_o}{c}\right)^{0.78} \qquad \text{for } d_c/D = 0.5 \qquad (9e)$$

Plot of the above equations and the finite element results are shown in Fig. 14. In general, the above equations could be expressed in the following form

$$k_s = a\left(\frac{h_o}{c}\right)^{b} \qquad (10)$$

It can be seen that constants a and b vary with different values of d_c/D. Therefore, it was decided to obtain a simple equation to express the relation between the constants (a and b) and the value of d_c/D. Plots of the constants, a and b, versus d_c/D are shown in Fig. 15. The following equations can be used to express the relation between a, b and d_c/D

$$a = 1.38 - 1.79\frac{d_c}{D} \qquad (11)$$

$$b = 3.64\left(\frac{d_c}{D}\right)^2 - 3.36\left(\frac{d_c}{D}\right) + 1.55 \qquad (12)$$

With Eqs. 11 and 12, it was decided to use a single equation (Eq. 10) which included the two main parameters c/h_o and d_c/D instead of using the five equations (Eqs. 9 a to e) with different values of d_c/D to predict the shear

buckling coefficients, k_s. The plot of Eq. 10 with constants a and b predicted by using Eqs. 11 and 12 are shown in Fig. 16 together with the shear buckling coefficient predicted by using the finite element method. It can be seen that the results of Eq. 10 compared well with the analytical results.

COMPARISON OF TEST RESULTS AND THE RESULTS OF MODIFIED PLATE EQUATION

With a given value of d_c/D and c/h_o, the shear buckling coefficients, k_s, can be obtained by using Eqs. 10 to 12. Then, the critical shear stress, τ_{cr}, can be evaluated by using Eq. 7. The critical reaction (R_{cr}) of local web buckling of coped I-beam is obtained by using Eq. 13.

$$R_{cr} = \tau_{cr} t_w (D - d_c) \tag{13}$$

where τ_{cr} = critical shear stress predicted by using Eq. 7 (and τ_{cr} should less than τ_y, the shear yield stress of web)

t_w = web thickness

D = beam depth

d_c = cope depth

The test results of the four specimens from this experimental program together with the three test results of the specimens from Cheng et al. (1984) are summarized in Table 3. The predictions which are obtained by the design equations (Eqs. 1 to 3) proposed by Cheng et al. (1984) and the present

proposed design equations (Eq. 13) are compared with the test results and are shown in Table 3. It can be seen that the results predicted by using Cheng's equations (Eqs. 1 to 3), R_{Cheng}, are very conservative. However, the results predicted by using the present proposed equation (Eq. 13), R_{cr}, are compared well with the test results. The test-to-predicted ratios varied from 0.92 to 1.06.

DESIGN EXAMPLE

For the purpose of illustration, consider the design of a cope beam with respect to local web buckling at coped section as shown in Fig. 17. This section and cope detail are identical to the test specimen RB12B by Cheng et al. (1984). The cope length (c) equals to 304.8 mm, cope depth (d_c) equals to 28.6 mm and the beam depth (D) equals to 303.8 mm. Therefore, the cope length to beam depth ratio is approximately equal to 1.1 and the cope depth to beam depth ratio is approximately equal to 0.1. The elastic modulus (E) is 205 GPa and the Poisson's ratio (ν) is 0.3 for structural steel member. The yield stress of the beam σ_y is 380 MPa.

By using the equation proposed in this report, the shear buckling coefficient, k_s, is calculated by the following equation

$$k_s = a\left(\frac{h_o}{c}\right)^b = 1.2\left(\frac{275.22}{304.8}\right)^{1.25} = 1.056$$

where $$a = 1.38 - 1.79\frac{d_c}{D} = 1.38 - 1.79 \times 0.1 = 1.2$$

$$b = 3.64\left(\frac{d_c}{D}\right)^2 - 3.36\left(\frac{d_c}{D}\right) + 1.55$$

$$= 3.64 \text{ x } 0.1^2 - 3.36 \text{ x } 0.1 + 1.55 = 1.25$$

$$h_o = D - d_c = 303.8 - 28.58 = 275.22 \text{ mm}$$

Then, the critical shear stress is calculated as

$$\tau_{cr} = k_S \frac{\pi^2 E}{12(1 - \nu^2)}\left(\frac{t_w}{h_o}\right)^2$$

$$= 1.056 \frac{\pi^2 \, 205000}{12(1 - 0.3^2)}\left(\frac{5.5}{275.22}\right)^2$$

$$= 78.14 \text{ MPa} < 0.577\sigma_y$$

Finally, the critical reaction is calculated as

$$R_{cr} = \tau_{cr} t_w (D - d_c)$$

$$= 78.14 \times 5.5 \times (303.8 - 28.58)$$

$$= 118.3 \text{ kN}$$

The corresponding test result, R_{max} (Cheng et al. 1984) is 122.3 kN, which is about 3% larger than the result from the proposed method.

SUMMARY AND CONCLUSIONS

Local web buckling behavior of coped I-beam was investigated both experimentally and analytically. In the experimental program, four full-scale tests on the local web buckling strength of coped steel I-beams were carried out.

The test results were compared with the predictions proposed by Cheng et al. (1984). It was found that Cheng's equation (Eq. 1) gave very conservative prediction, especially when d_c/D was small.

The finite element program, ABAQUS (1997), was employed to analyze the test specimens. In general, the finite element analysis results were in good agreement with the test results. Both test and analytical results showed that the buckling line at the coped region inclined at an angle when the cope length to the reduced beam depth was small ($c/h_o<1.5$). Therefore, it was believed that the shear stresses dominated the buckling behavior when the ratio of cope length to the reduced beam depth was small. Hence, a modified plate model was proposed to predict the LWB strength of coped I-beam. The results of the modified plate model were compared well with the test results and the test-to-predicted ratios varied from 0.95 to 1.01.

Based on the proposed modified plate model, parametric studies were conducted to examine the effects of the cope length to the reduced beam depth ratio, cope depth to beam depth ratio and thickness of the web. It was found that the local web buckling strength of coped section decreased as cope depth and cope length increased and the amount of reduction of the local web buckling strength of coped section were different for different values of cope depth to beam depth ratios.

With the results of the parametric studies, a modified plate buckling equation (Eq. 13) that considered the shear buckling phenomenon was proposed to predict the local web buckling strength of coped section. The results of the proposed equation compared well with the test results from this study (Yam et al. 2000) and from Cheng et al. (1984). The test-to-predicted ratios varied from 0.92 to 1.06.

ACKNOWLEDGEMENTS

The authors would like to extend their gratitude to the Research Committee of the University of Macau in providing financial support to this project. The assistance of the technical staff of the Bridge and Structural Laboratory at the SouthWest JiaoTong University, China, is acknowledged.

APPENDIX I. REFERENCES

ABAQUS (1997) "User's manual-version 5.8.", Hibbit, Karlsson & Sorenson, Pawtucket, R.I.

American Society for Testing and Materials (1997) "A370 Standard Test Methods and Definitions for Mechanical Testing of Steel Products." Philadelphia, PA.

Birkemoe, P.E. and Gilmor, M.I. (1978) "Behavior of Bearing Critical Double Angle Beam Connections." *Engineering Journal*, AISC, Vol. 15, No. 4, 109-115.

Cheng, J.J.R., and Yura, J.A. (1986) "Discussion of Buckling of coped steel beams." *J. Struct. Division,* ASCE, **112**: 201-203.

Cheng, J.J.R., Yura, J.A., and Johnson, C.P. (1984) "Design and behaviour of coped beams." *Ferguson Structural Engineering Laboratory Report No. 84-1,* The University of Texas at Austin.

Cheng, J.J.R., and Yura, J.A. (1986) "Local web buckling of coped beams." *J. Struct Division*, ASCE, **112** :2314-2331.

Cheng, J.J.R. and Snell, W.J. (1991) "Experimental study of lateral buckling of coped beams." *Proceedings, Structural Stability Research Council*, *Annual Technical Session,* Chicago, Illinois: 181-192.

Cheng, J.J.R. (1993) "Design of steel beams with end copes." *J. Construct. Steel Research*, **25** : 3-22.

"Joints in simple construction, Volume 1: Design methods" (1993) 2nd ed., British Constructional Steelwork Association Limited.

Lam, C.C., Yam, M.C.H. and Iu, V.P. (1998) "Analytical study of the elastic lateral torsional buckling of coped I-beam." *FST Report No. CE-1998-02(ST),* Faculty of Science and Technology, University of Macau.

Lam, C.C., Yam, M.C.H., Iu, V.P. and Cheng, J.J.R. (2000) "Design for lateral torsional buckling of coped I-beams." *J. Construct. Steel Research*, **54(3)**, 423-443.

Ricles, J.M. and Yura, J.A. (1980) "The Behavior and Analysis of Double-Row Bolted Shear Web Connections." Dept. of Civil Engineering, *Phil. M. Ferguson Structural Engineering Laboratory Thesis No. 80-1*, The University of Texas at Austin, September.

Steelwork Design Guide to BS 5950: Part 1 and Part 2:1990, Volume 1 Section properties member capacities, (1996), 4th Edition, Ascot, Steel Construction

Yam, M.C.H. and Cheng, J.J.R. (1990) "Fatigue strength of coped steel beams." *J. Struct. Division*, ASCE, **114**: 16-30.

Yam, M.C.H. , Lam, A.C.C., Iu, V.P. and Cheng, J.J.R. (2000) "Experimental Investigation of the Local Web Buckling strength of Coped Steel I-Beam." *Canadian Society for Civil Engineering, 2000 Conference Proceedings,* 105-113.

APPENDIX II. NOTATION

a_T	=	Transverse length of plate
c	=	Cope length
D	=	Beam depth
d_c	=	Cope depth
E	=	Modulus of Elasticity
e	=	Initial imperfection
f	=	Adjustment factor
h_o	=	Height of web of T-section
I_I	=	Moment of inertia of I-section
I_T	=	Moment of inertia of T-section
k	=	Plate buckling coefficient
k_s	=	Shear buckling coefficient
m	=	τ_T/τ_I
R	=	Reaction at cope
R_{cr}	=	Critical reaction
S_{Tee}	=	Elastic section modulus of T-section
t	=	Thickness of plate
t_w	=	Web thickness
$\bar{y}$	=	Neutral axis of T-section measured from the extreme fiber of the flange
ν	=	Poisson's ratio
τ_{cr}	=	Critical shear stress
τ_I	=	Shear stress of I-section at the bottom flange/web junction
τ_T	=	Shear stress at the cope
σ_{cr}	=	Plate critical stress
σ_y	=	Static yield stress

Table 1. Cross-section dimensions of I-section and cope details

Specimen	Beam depth (D) mm	Cope length (c) mm	Cope depth (d_c) mm	d_c / D
406d005	398	342.9	19.9	0.05
406d01	398	342.9	39.8	0.1
406d03	398	342.9	119.4	0.3
457d02	450	388.0	90.0	0.2

Table 2. Comparison of test results and present design method

Specimens	P_{Test} (kN)	P_{FEM} (kN)	$\frac{P_{FEM}}{P_{Test}}$	R_{Test} (kN)	R_{Cheng} (kN)	R_{Design} (kN)	$\frac{R_{Test}}{R_{Cheng}}$	$\frac{R_{Test}}{R_{Design}}$
406d005	248.8	250.5	1.01	165.9	135.1	135.1	1.23	1.23
406d01	241.6	242.4	1.00	161.1	126.5	126.5	1.27	1.27
406d03	167.9	159.6	0.95	111.9	101.3	101.3	1.10	1.10
457d02	403.3	404.0	1.00	268.9	222.1	222.1	1.21	1.21

R_{Test} : Test reaction at end plate
R_{Cheng} : Elastic buckling reaction of end plate according to the critical stress at cope predicted by Eqn. 1
R_{Design} : The lowest value of R_{vy}, R_v and R_{Cheng} (R_{vy} and R_v were not shown in the table)

Table 3. Comparison of test results, results predicted by Cheng and results predicted by the modified plate equation

Specimens	R_{Test} (kN)	R_{Cheng} (kN)	R_{cr} (kN)	$\frac{R_{Test}}{R_{Cheng}}$	$\frac{R_{Test}}{R_{cr}}$
406d005	165.9	135.1	164.88	1.23	1.01
406d01	161.1	126.5	152.43	1.27	1.06
406d03	111.9	101.3	108.73	1.10	1.03
457d02	268.9	222.1	255.76	1.21	1.05
*RB12B	122.3	93.0	118.85	1.32	1.03
*RB12C	73.4	53.0	71.58	1.38	1.03
*RB12D	56.9	40.94	61.49	1.39	0.92

* RB12B, RB12C and RB12D are the test results from Cheng et al. (1984)

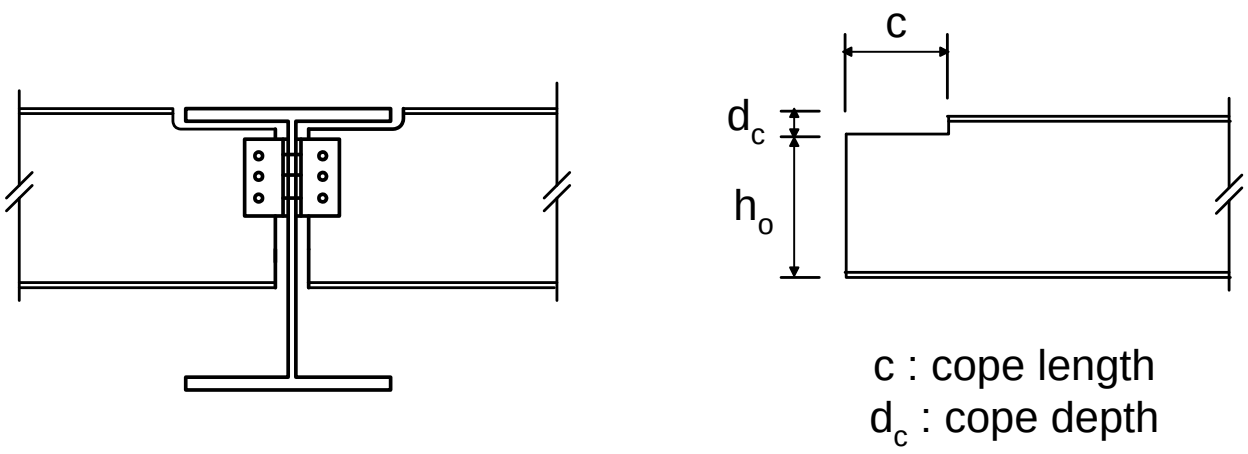

Fig. 1 Top flange coped I-beam

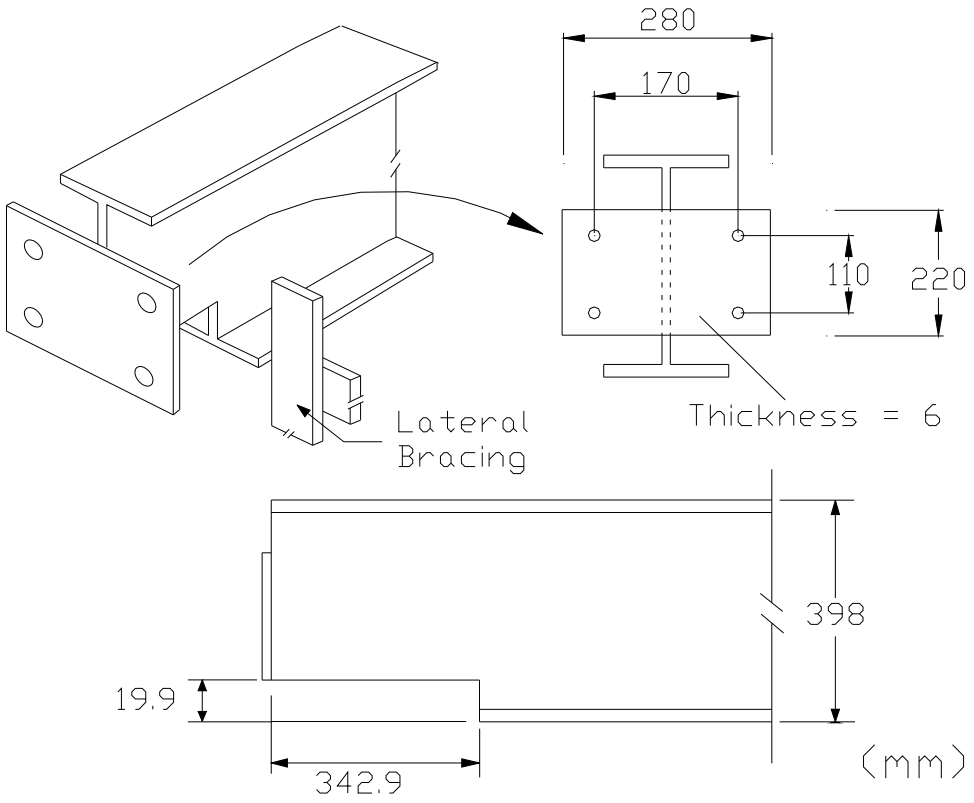

Fig 2. Typical cope details and dimensions of end plate of 406d005

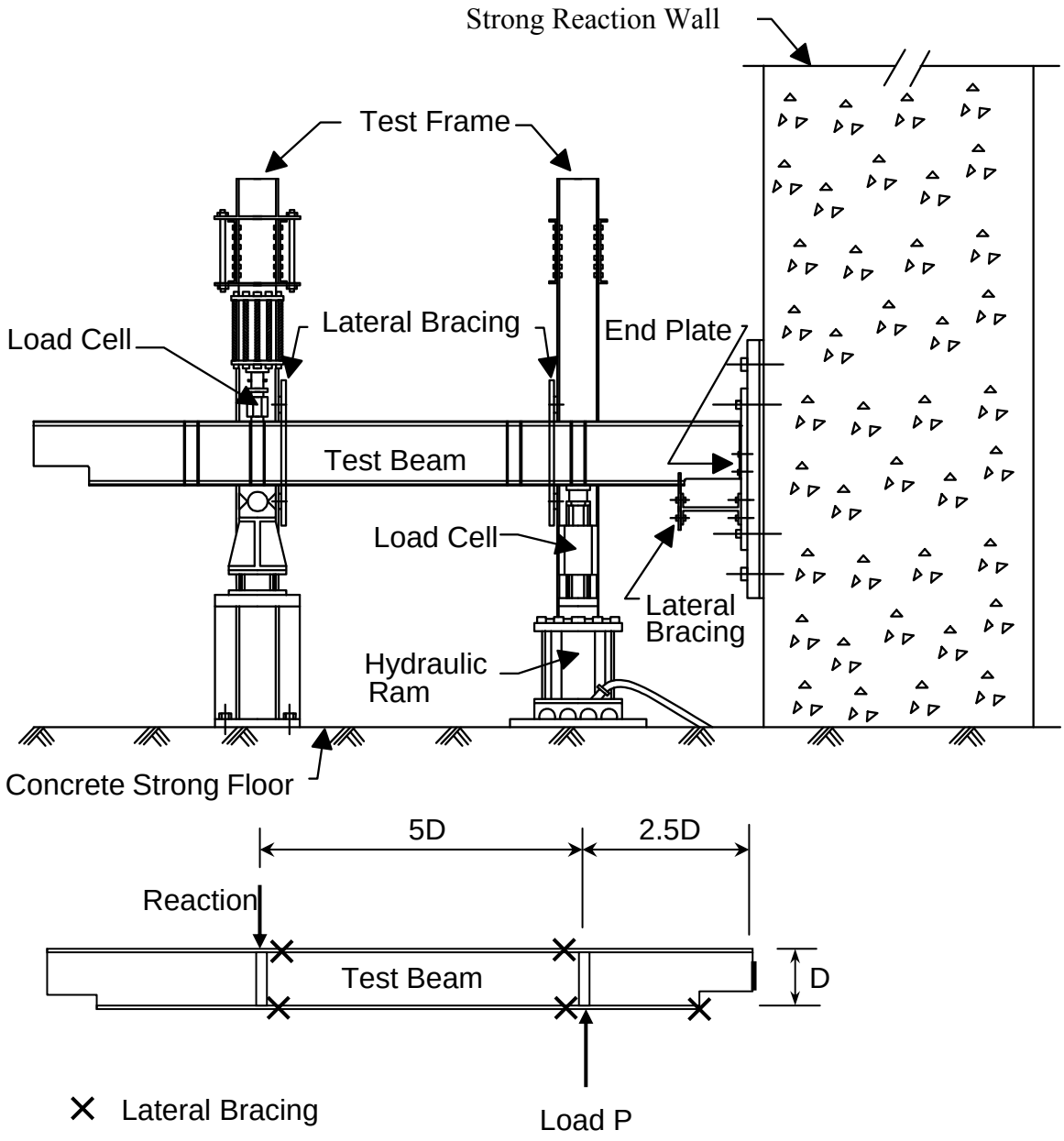

Fig. 3 Test setup and test specimen

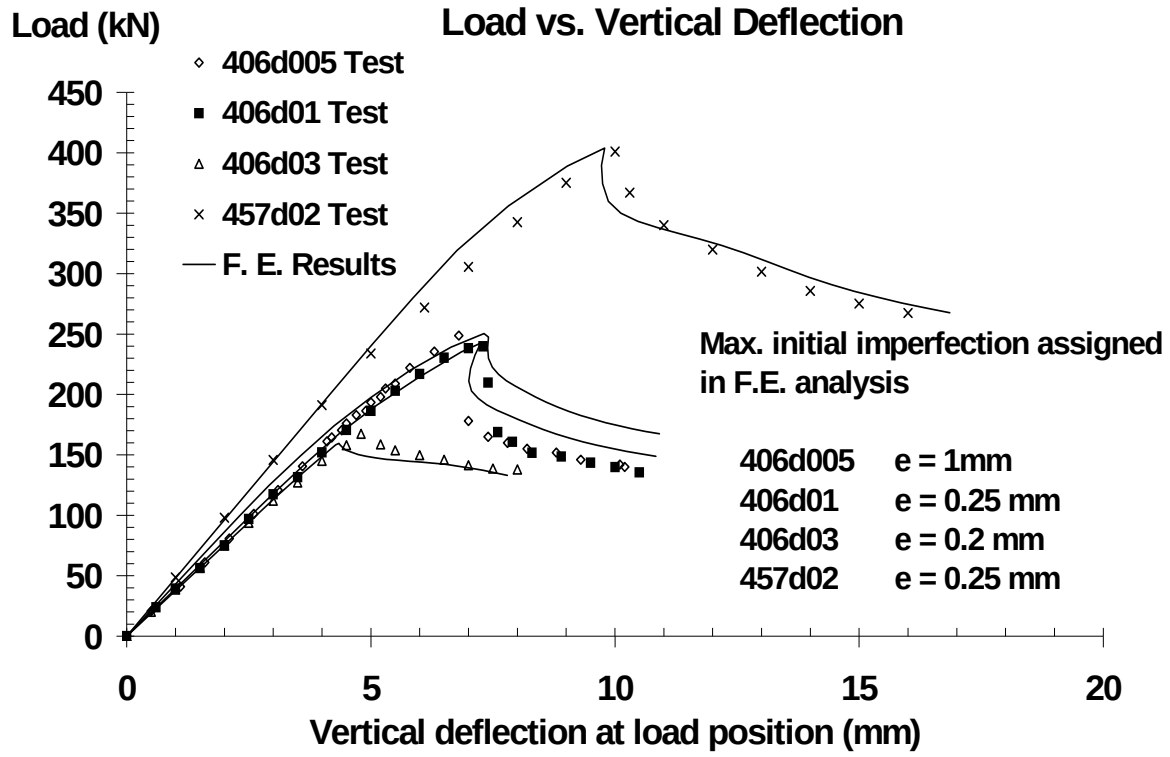

Fig. 4 Comparison of load vs. vertical deflection curves of finite element results with test results

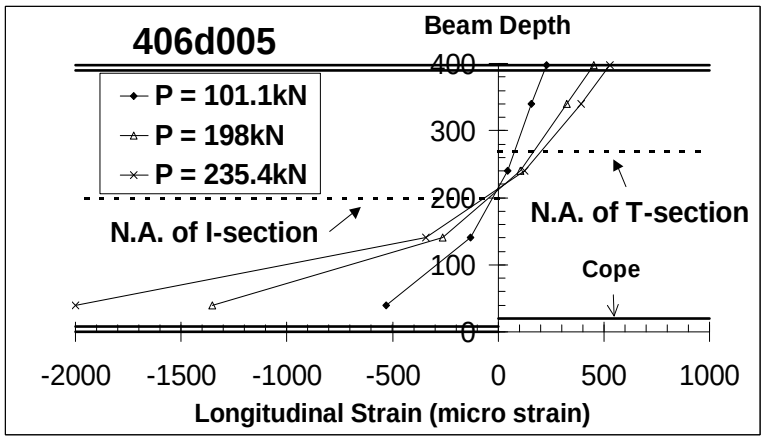

(a) 406d005

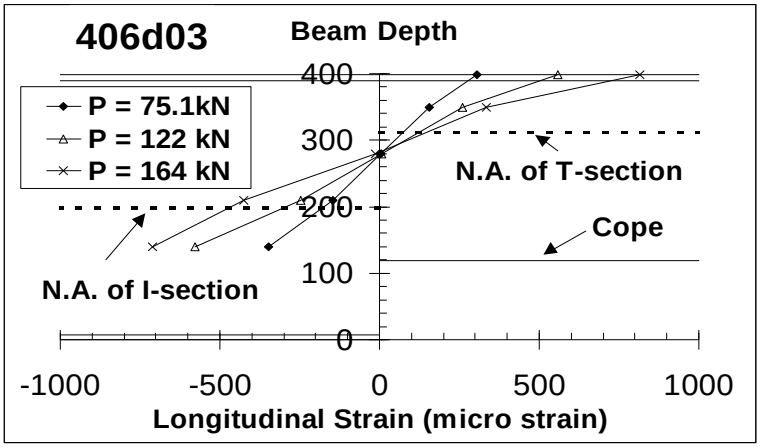

(b) 406d03

Fig. 5 Strain readings at the junction of I-section and T-section of specimens 406d005 and 406d03

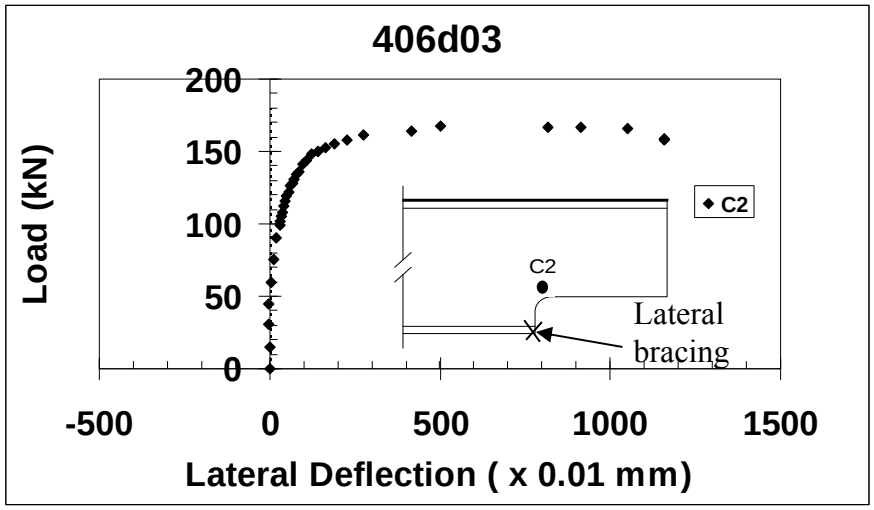

Fig. 6 Load versus out-of-plane deflection of point C2 of specimen 406d03

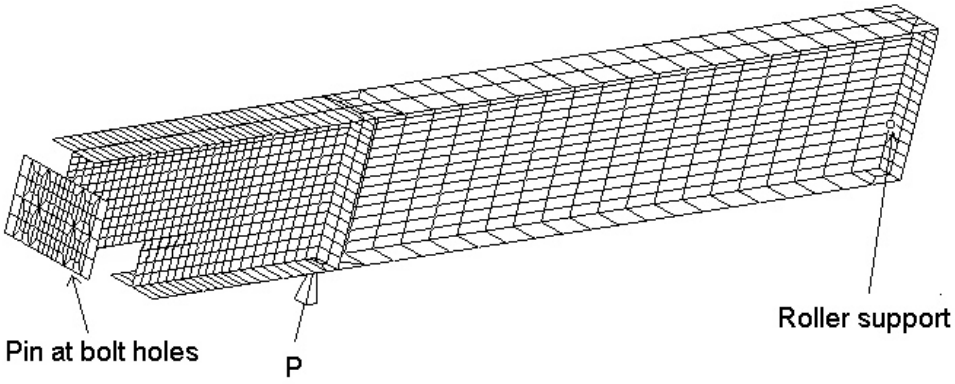

Fig. 7 Finite element model of coped I-beams

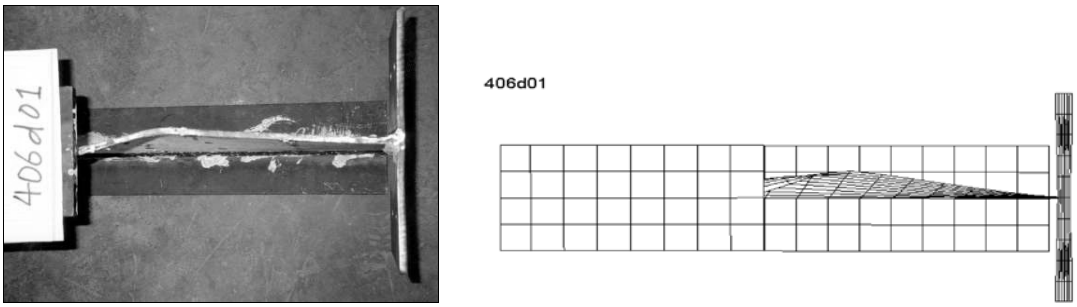

Fig. 8 Comparison of experimental buckled shape and finite element results of specimen 406d01 (deflected shape at cope line – bottom view)

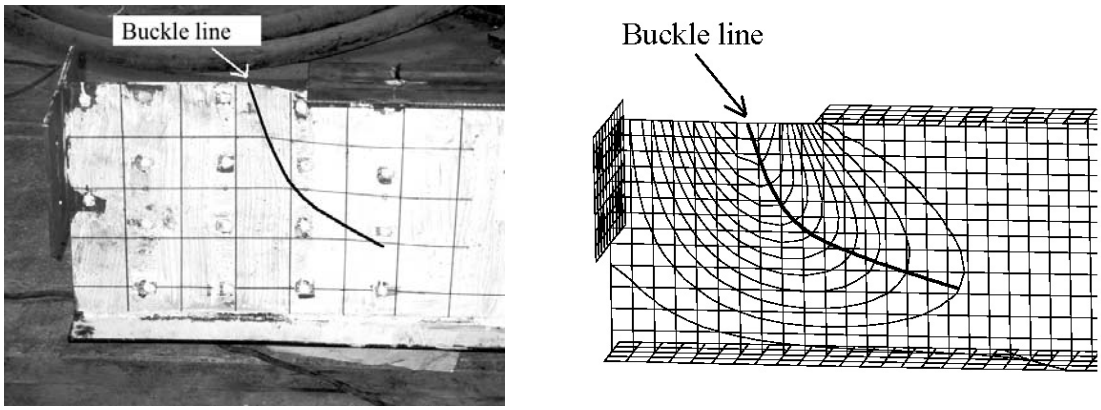

(a) Test result (b) Contour plot of out-of-plane deflection

Fig. 9 Test and finite element results of buckled shape of specimen 406d005

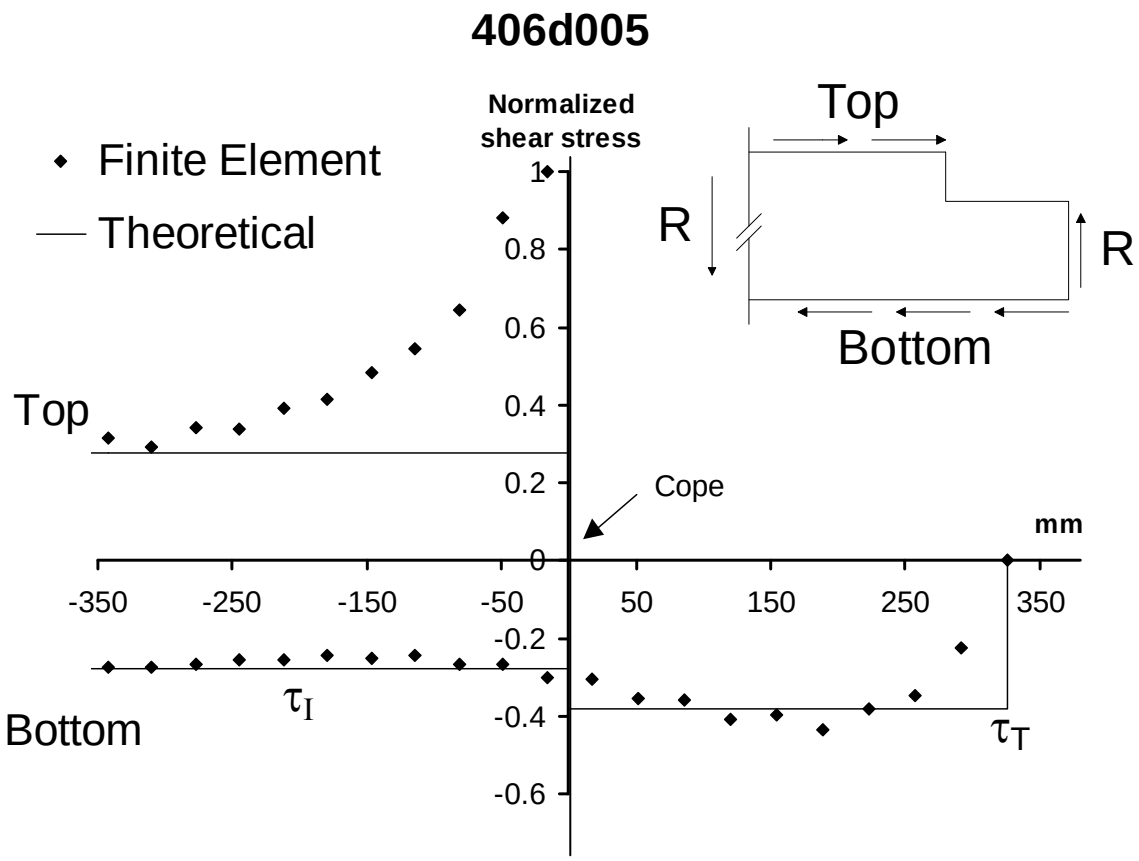

Fig. 10 Comparison of shear stress at flange/web junction of finite element results and theoretical results of specimen 406d005

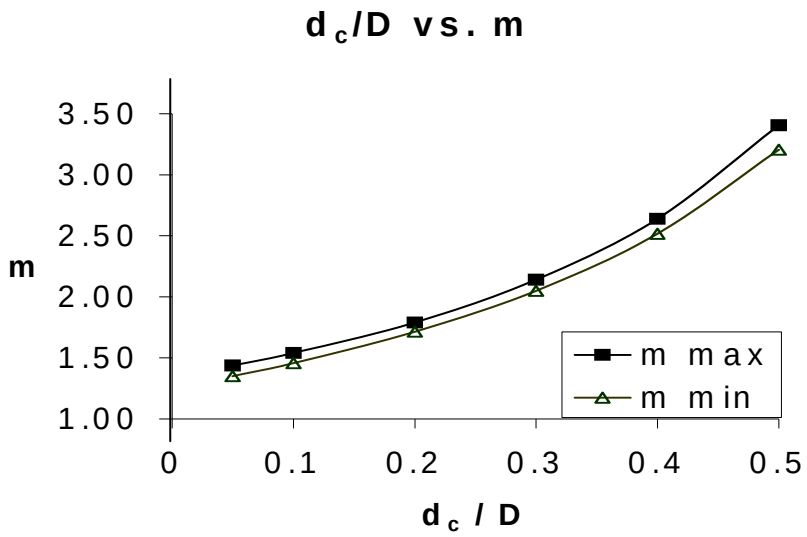

Fig. 11 d_c/D versus shear stress factor (m)

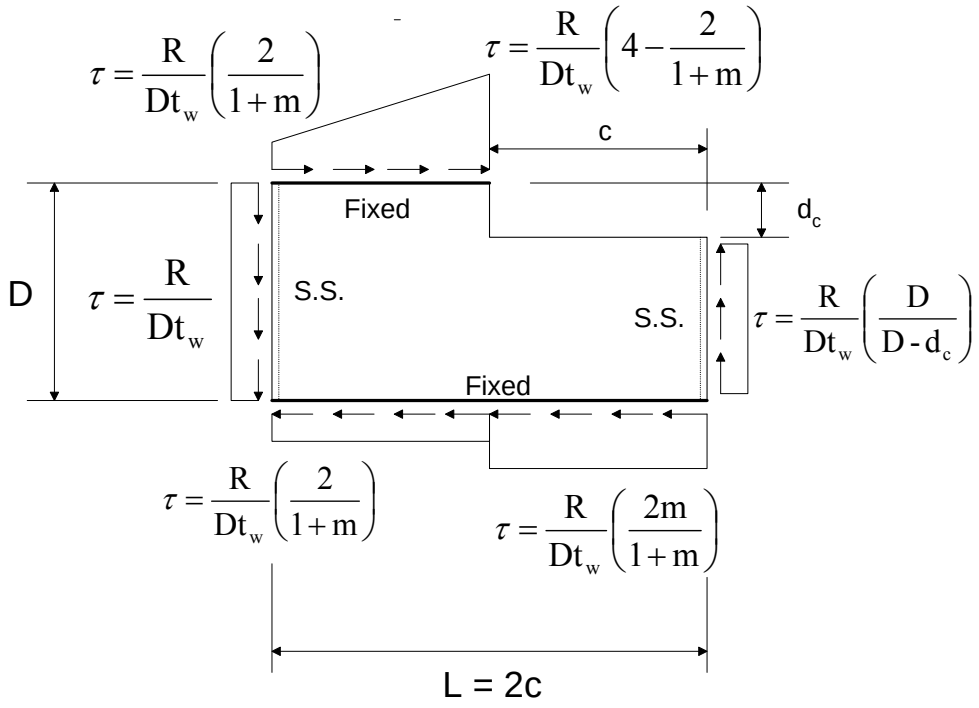

Fig. 12 Plate model with shear as boundary stress

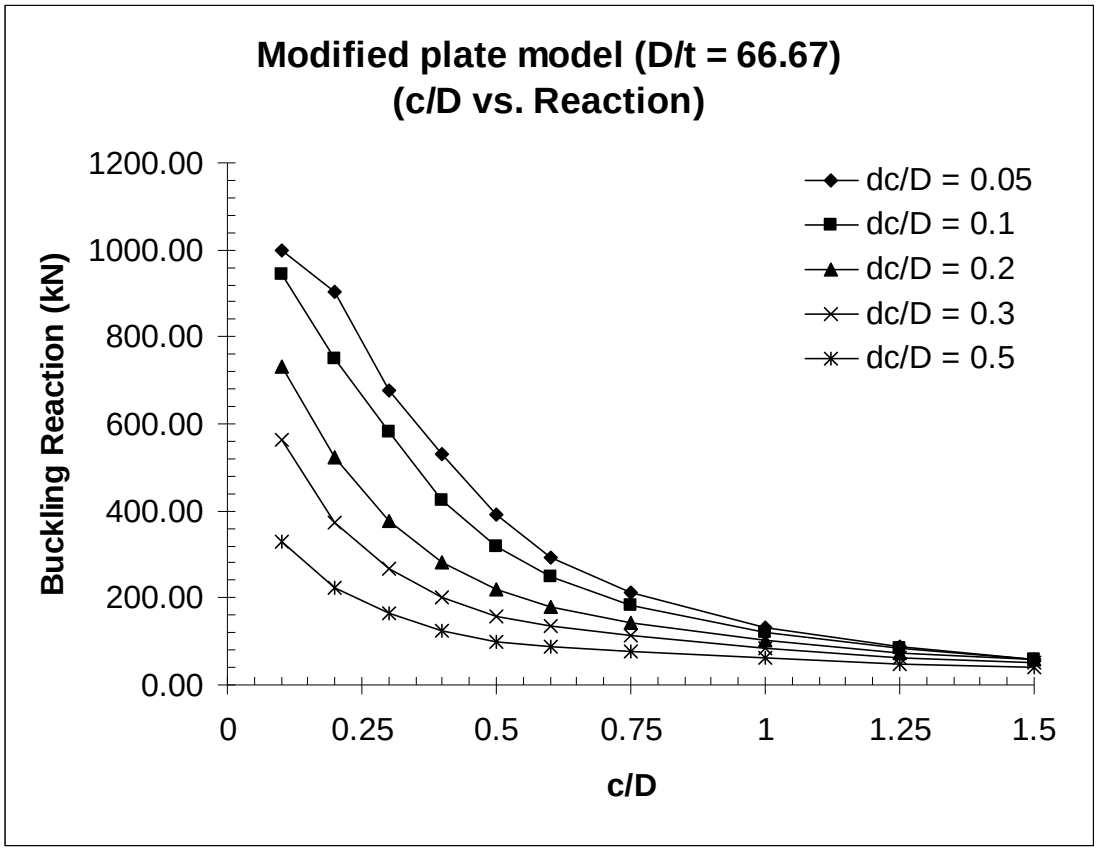

Fig. 13 Buckling reaction of modified plate model versus c/D with various d_c/D ratios

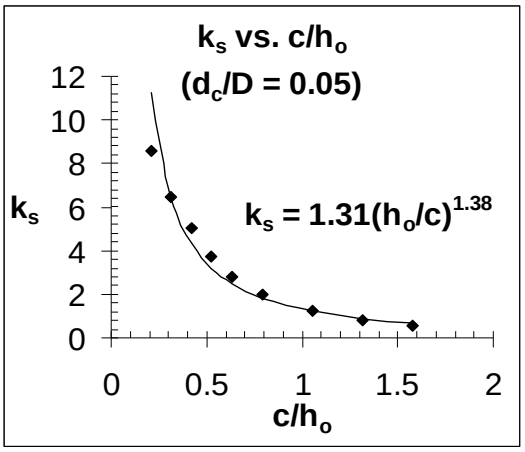

(a) $d_c/D = 0.05$

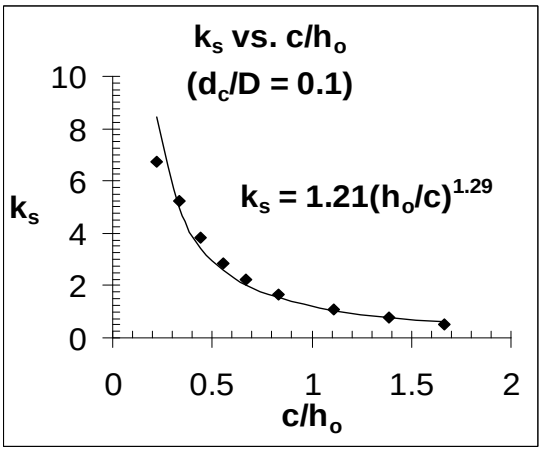

(b) $d_c/D = 0.1$

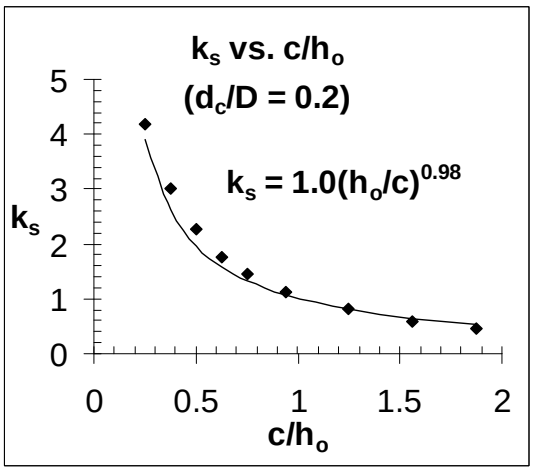

(c) $d_c/D = 0.2$

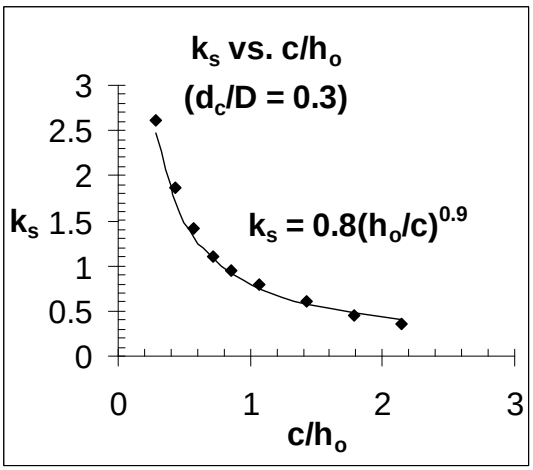

(d) $d_c/D = 0.3$

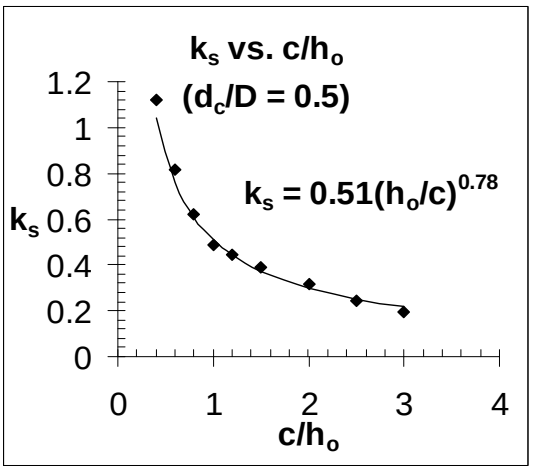

(e) $d_c/D = 0.5$

Fig. 14 Equations in power order form for predicting the shear buckling coefficient, k_s, with different d_c/D

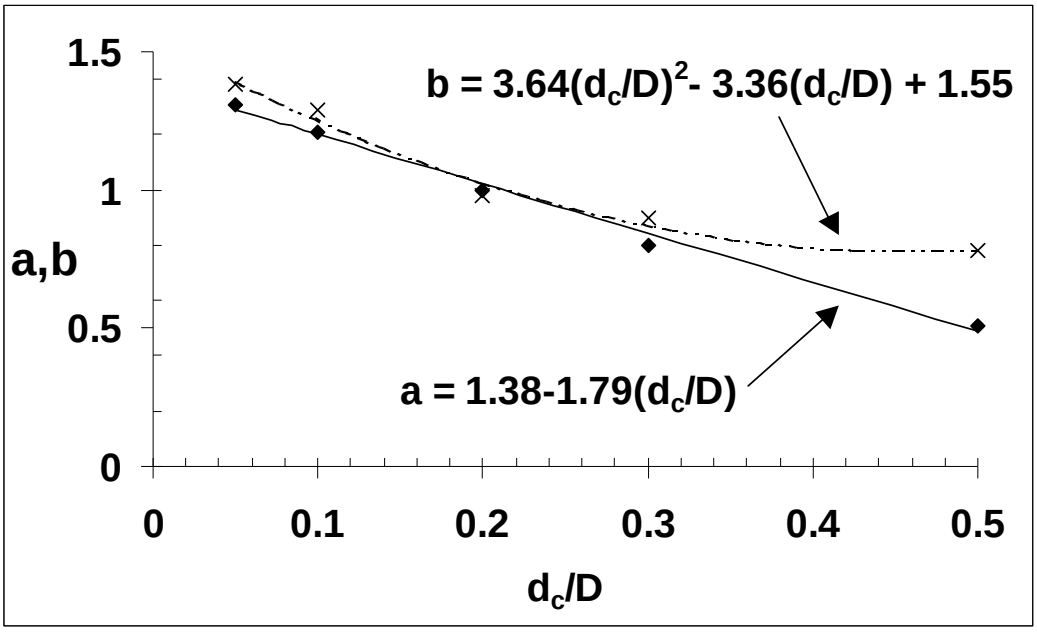

Fig. 15 Coefficients, a and b, versus d_c/D

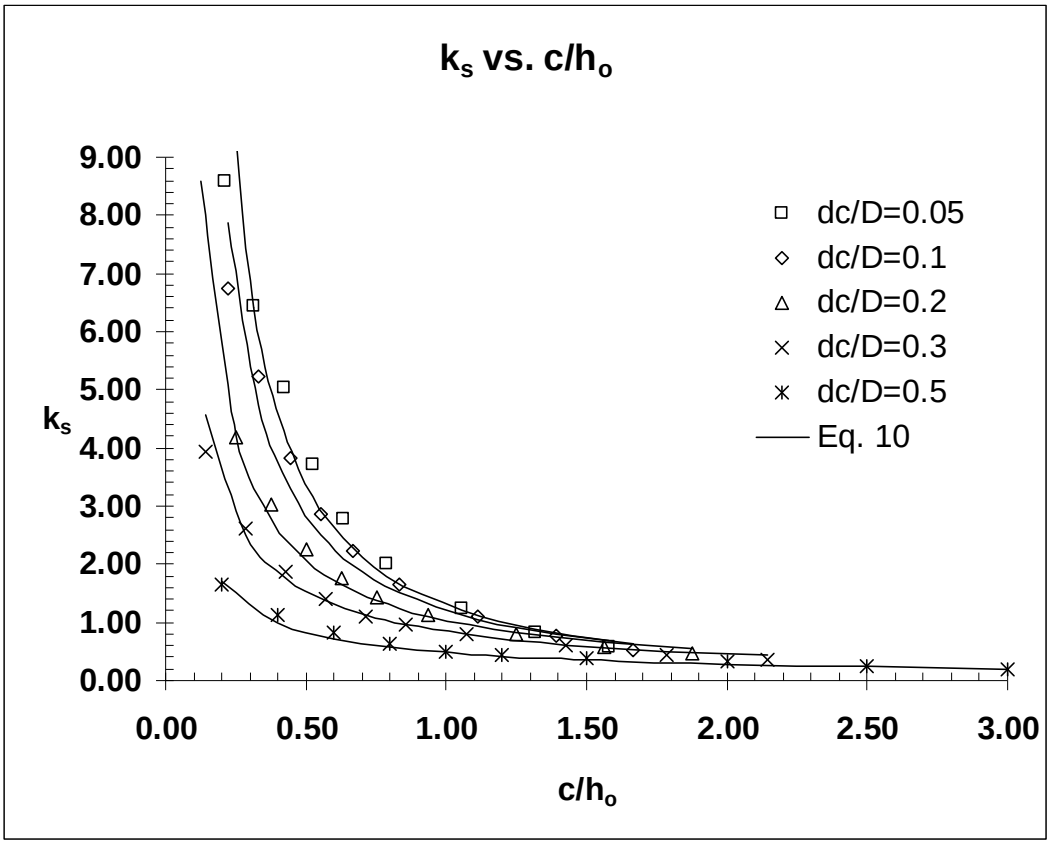

Fig. 16 Comparison of the shear buckling coefficients, k_s, predicted by using Eq. 10 and the finite element results

R

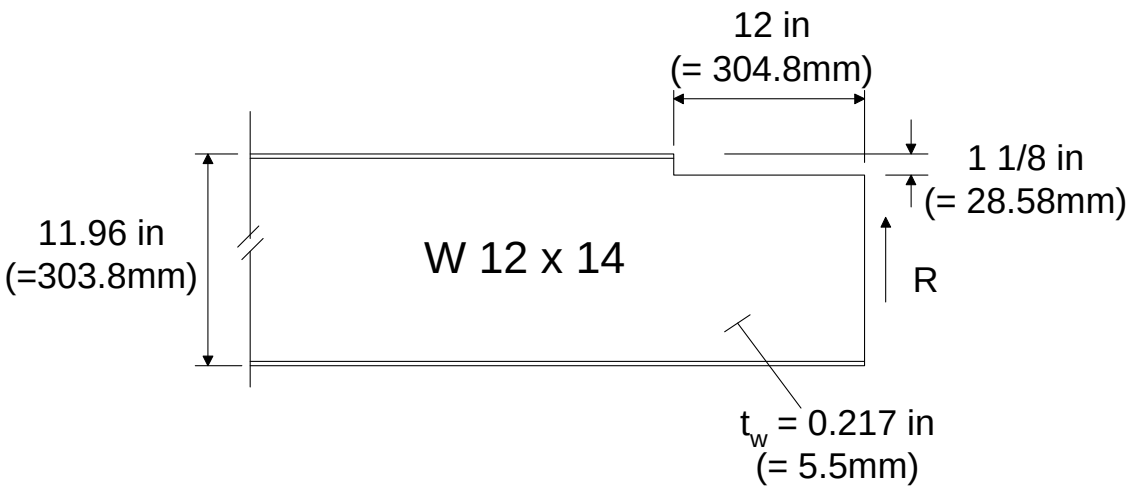

Fig. 17 Design example of coped steel I-beam for local web buckling